Islamic Azad University

Journal of
Optoelectronical Nanostructures

Spring 2022 / Vol. 7, No. 2

## Research Paper

# Nonlinear Energy Exchange between Solitons in Modes of a Silica Few-Mode Fiber

**Saba Parva[1], Mohsen Hatami*,[1]**
[1] Faculty of Physics, shiraz University of Technology, Shiraz, Iran

**Received:** 9 Feb. 2022
**Revised:** 25 Mar. 2022
**Accepted:** 26 Apr. 2022
**Published:** 15 Jun. 2022

**Use your device to scan and read the article online**

**Keywords:**
**All-Optical Switching, Bright Soliton, Cross Phase Modulation, Few Modes Fiber, Nonlinear Silica Fiber.**

**Abstract:**
Recently soliton propagation in few-mode fiber has been studied. In this paper, we used commercially few-mode fiber for investigating the soliton propagation. Three modes exist in this fiber, by considering polarization, we have six propagation modes. Initially, we calculate the propagation mode, effective cross-section, and dispersion for each mode then soliton propagation in fiber modes with respect to phase are simulated. The nonlinear effect causes XPM which affects propagation modes to each other. By various values of phase, the first maximum energy transfer between modes is calculated. We find minimum normalized length 0.66 which equal to a length of 23.3 meters of silica fiber for energy exchange. The energy exchange can be used as a basis for all-optical switching. Interestingly, these effects cause energy transfer between different modes and strongly depend on the phase difference. So, the results of this simulation can be used to design all-optical self-switches and all optical logic gates.

Citation: Saba Parva, Mohsen Hatami. Nonlinear Energy Exchange between Solitons in Modes of a Silica Few-mode Fiber. **Journal of Optoelectronical Nanostructures. 2022; 7 (2): 64-78 DOI: 10.30495/JOPN.2022.29968.1259**

***Corresponding author:** Mohsen Hatami
**Address:** Department of Physics, Shiraz University of Technology, Shiraz, Iran.
**Tell:** 09131518991 **Email:** hatami@sutech.ac.ir

## INTRODUCTION

Because of small optical effective mode area of single-mode fibers, they have been used for designing nonlinear all-optical devices [1] such as light communication systems and network [2-6]. Multimode and few mode fibers are recently used for linear optical communication channels and multiplexed to increase capacity [7-10]. Recently propagation of solitons in nonlinear multimode fibers has been subject of many investigations [11-20]. Such fibers have new features that can exchange energy between modes of fiber via cross phase modulation (XPM). In this letter we consider a commercial few-mode fiber and investigate the propagation of fundamental soliton in six modes with nonlinear effects. Here we simulate our calculations by introducing a set of nonlinear Schrodinger equations that coupled to each other are numerically solved by a combination of finite difference method and Runge-Kutta method. We study the evaluation of fundamental bright solitons in different modes of a few-mode fiber and study their effects on each other as well as the energy exchange between them.

## FIBER MODES

Here we have used step-index few-mode fiber from YOFC. Whose parameters are given in Table I. We use characteristic equation for weakly guiding fiber to find fiber modes [21]:

$$\frac{(pa)J'_m(pa)}{J_m(pa)} = \frac{(qa)K'_m(qa)}{K_m(qa)} . \tag{1}$$

Where 2a is core diameter, p and q are defide as:

$$p = \sqrt{n_1^2 k_0^2 - \beta^2} , \qquad q = \sqrt{\beta^2 - n_2^2 k_0^2} . \tag{2}$$

Where $n_1$ and $n_2$ are refractive index of core and clad respectively. $\beta$ is propagation constant and $k_0 = 2\pi/\lambda_0$.

 DOI: 10.30495/JOPN.2022.29968.1259

TABLE I.
PARAMETERS OF COMMERCIAL SILICA FIBER FROM YOFC

| Fiber Type | | FM SI-2 | |
|---|---|---|---|
| **Part No.** | | FM2010-B | |
| Optical Charac.@1550nm | | Range | Typical Value |
| Core Diameter (μm) | | 14.0 ± 0.5 | -- |
| Core Refractive Index | | 1.4485 | -- |
| Cladding Diameter (μm) | | 125.0 ± 0.7 | -- |
| Cladding Non-circularity (%) | | < 0.7 | -- |
| Coating Diameter (μm) | | 245.0 ± 10.0 | -- |
| Dispersion (ps/(nm·km)) | LP01 | < 22 | 21 |
| | LP11 | < 21 | 19.5 |
| Dispersion Slope (ps/($nm^2$·km)) | LP01 | < 0.1 | 0.08 |
| | LP11 | < 0.1 | 0.07 |
| Effective Area ($\mu m^2$) | LP01 | > 100 | 130 |
| | LP11 | > 200 | 220 |
| Attenuation (dB/km) | LP01 | < 0.21 | 0.19 |
| | LP11 | < 0.21 | 0.19 |
| Differential Group Delay (ps/m) | LP11-LP01 | < 2.1 | 1.9 |

We numerically solve the charactristic equation to obtain the propagation constant $\beta$ and dispersion, by using MATLAB software. Propagation constant and dispersion of order of 1,2 in term of wavelenght for two modes $LP_{01x}$ and $LP_{11\,x}$ are calculated numerically and the result are shown in Figures 1 and 2. According to the numerical studies, this fiber has three propagation modes in the telecommunication wavelength $\lambda_0 = 1.55\ \mu m$ which has six independent modes by considering X and Y polarization. By using the solution of Eq. 1 we numerically calculate the propagation constant of modes, effective cross section and scattering.

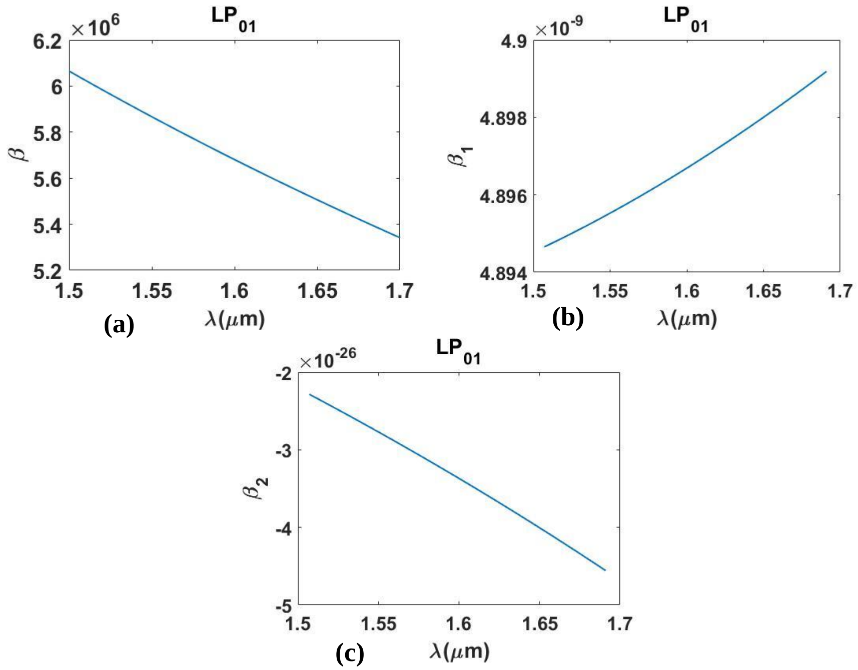


**Fig. 1.** a) Propagation constant b) first order dispersion c) second order dispersion (GVD) for $LP_{01}$ mode

Propagation constant and different order of dispersion for silica fiber in telecommunication wavelength for $LP_{01}$ and $LP_{11}$ modes are brought in "Table II". As we expected, the dispersion of $LP_{01}$ mode is negative at communication wavelength $\lambda_0 = 1.55\mu m$ which is suitable for bright soliton propagation that is shown in Fig. 1(c). Also, in Fig. 2 (c) the dispersion is negative at communication wavelength and very close to the value of dispersion in $LP_{01}$ mode.

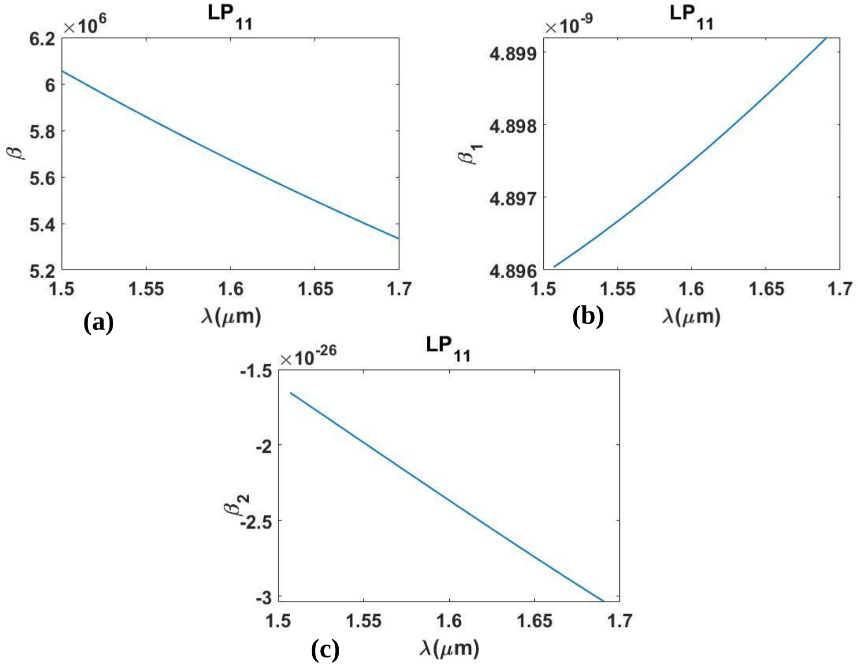


**Fig. 2.** a) Propagation constant b) First order dispersion c) Second order dispersion (GVD) for $LP_{11}$ mode.

**TABLE II**
**PROPAGATION CONSTANT AND DISPERSION**

| | $\beta$ | $\beta_1$ | $\beta_2$ |
|---|---|---|---|
| $LP_{01}$ | $(5.87 \times 10^{6}\ 1/m)$ | $(0.49 \times 10^{-08}\ s/m)$ | $(-0.29 \times 10^{-25}\ s^2/m)$ |
| $LP_{11a,}LP_{11b}$ | $(5.86 \times 10^{6}\ 1/m)$ | $(0.49 \times 10^{-8}\ s/m)$ | $(-0.20 \times 10^{-25}\ s^2/m)$ |

Different values of propagation constant and dispersion of orders 1 and 2 at telecommunication wavelength 1.55 are given in Table II for silica fiber. The value of propagation constant for $LP_{11a}$ and $LP_{11b}$ are exactly same as each other and the value of dispersions. We will use the parameters in Table II for simulating the propagation of soliton in the next section.

## NONLINEAR EQUATIONS

Here the extended nonlinear Schrödinger coupling equations for multimode fiber are bring as [1]:

$$\frac{\partial u_p}{\partial \xi} + d_{1p}\frac{\partial u_p}{\partial \tau} + i\frac{d_{2p}}{2}\frac{\partial^2 u_p}{\partial \tau^2} = iN_1^2 \times \sum_l \sum_m \sum_n f_{lmnp}\left[\frac{2}{3}(u_l^H u_m)u_n + \frac{1}{3}(u_n^T u_m)u_l^*\right] e^{i\Delta\beta_{lmnp}L_D\xi} \quad (3)$$

Where $p, l, m, n = 1,2,3$ subscripts T refers to transpose and H for Hermitian conjugate of $u_p = \frac{A_p}{\sqrt{P_1}}$ where $u_p$ is a column matrix. $A_p$ refers to the polarized Jones vector, $A_p = \left[A_{px}, A_{py}\right]^T$ . $A_{px}$ and $A_{py}$ are the slowly varying envelope of the x-polarized pulse propagation in $p$th spatial mode of the fiber. $P_1$ is used for normalizing the peak power needed for fundamental soliton in the $LP_{01}$ mode. Mode dispersion length is defined as $L_D = T_0^2/|\beta_{21}|$, for normalizing the propagation length, where $\xi = z/L_D$. Also, $\tau = t/T_0$ is the normalized time, where $T_0$ is input pulses width.

In Eq. 3 the propagation constant $\beta_p$ of individual mode was obtained by Taylor series as:

$$\beta_p(\omega) = \beta_{0p} + \beta_{1p}(\omega - \omega_0) + \beta_{2p}(\omega - \omega_0)/2 + \cdots \quad (4)$$

Where $\beta_{kp} = \left(\frac{d^k\beta_p}{d\omega^k}\right)\Big|_{\omega = \omega_0}$. The parameters $d_{1p}$, and $d_{2p}$ are defined as [12]:

$$d_{1p} = (\beta_{1p} - \beta_{11})L_D/T_0,\ \ d_{2p} = \beta_{2p}/|\beta_{21}|. \quad (5)$$

The $LP_{11a}$ and $LP_{11b}$ modes, are degenerated so, $d_{k2} = d_{k3}$, $d_{11} = 0$ and $d_{21} = -1$ (for anomalous dispersion), the other parameters should be calculated.

for the dispersive effects, namely $d_{12}$ and $d_{22}$. We ignore dispersions that higher than third order for this work and focused on the intermodal cross-phase coupling. The right side of Eq. 3 is pointed to phase mismatch is given by $\Delta\beta_{lmnp} = \beta_{0m} + \beta_{0n} - \beta_{0l} - \beta 0p$. In Eq. 3, soliton order $N_1$ is defined as $N_1^2 = \gamma P_1 T_0^2 / |\beta_{21}|$, where $\gamma$ is the nonlinear parameter. The following integral stands for intermodal nonlinear dimensionless coupling $f_{lmnp}$:

$$f_{lmnp} = A_1^{eff} \iint F_l^* F_m F_n F_P^* dxdy, \tag{6}$$

Where $F_p(x, y)$ is the transverse distribution of the $p$th mode, which satisfies $\iint |F_m|^2 (x, y) dxdy = 1$. By this definition we have $f_{1111} = 1$. The values of $l$, $m$, $n$, $p$ can vary from 1 to 3, one should be calculated 81 parameters. We numerically calculate all intermodal nonlinear cross-phase coupling. Because of the orthogonality of modes, most of them are zero. There are 19 nonzero terms. For example, $f_{2222} = f_{3333} = 0.5783$ and here $T_0 = 1\,ps$ and $L_D = 34.88\,m$. The input of each mode is in the form of fundamental bright solitons $u(0, \tau) = u_0\, sech(\tau)$, when no soliton is lunched to a mode $u_0$ is considered $u_0 = 0$.

## SIMULATION

As we noted above, we have used step-index few-mode fiber from YOFC, whose parameters are given in Table I. According to the numerical studies, this fiber has three propagation modes in the telecommunication wavelength $1.55\mu m$ which has six independent modes by considering X and Y polarization. By simulating “Eq. 3”, we investigate the propagation of fundamental soliton in different fiber modes and their interaction. By using the parameters obtained from the tables related to the three-mode silica fiber, we simulate the pulse propagation in this fiber. The soliton input of each mode is defined as $u(0, \tau) = u_0 sech(\tau)$. And the normalized energy of soliton for each mode is defined as follows:

$$Energy(z) = \int_{-\infty}^{+\infty} u(z, \tau) d\tau \tag{7}$$

Here $u_0$ set to zero for modes in which no soliton is launched and for fundamental soliton is one. Other parameters required for the simulation are given in the Table III.

**TABLE III**
**SOME PARAMETERS REQUIRED FOR SIMULATEION**

| | $\gamma$ | $n_2^I$ | $T_0$ | $L_D$ | v |
|---|---|---|---|---|---|
| **Bright soliton** | $8.02^{-4} W^{-1}/m$ | $2.7 \times 10^{-20}$ $m^2/w$ | $10^{-12}s$ | $35.38\,m$ | 3.30 |

Eq. 3 is six coupled equations that must be given six soliton inputs then we examine the interaction between modes, which is only through XPM. It should be noted that if the nonlinear effect is not considered, modes are propagation independently and without any interaction. In order to be able to accurately study the interaction between modes, we investigate different types of modes. First, we assume that the fundamental soliton input amplitude for $LP_{01x}$ mode is one and the other amplitude are zero. Fig 3 (a) shows the soliton propagation and Fig 3 (b) shows the energy of each mode up to 3 times of scattering length. As shown in the figure, the energy of the $LP_{01x}$ mode remains unchanged and the soliton continues to move without changing its shape, and no energy exchange takes place with the other modes. In the same way as the soliton form in Fig 3 (a), the intensity at the center of the pulse is at a maximum, and gradually this intensity decreases at the sides and propagates without change in the direction of the fiber.

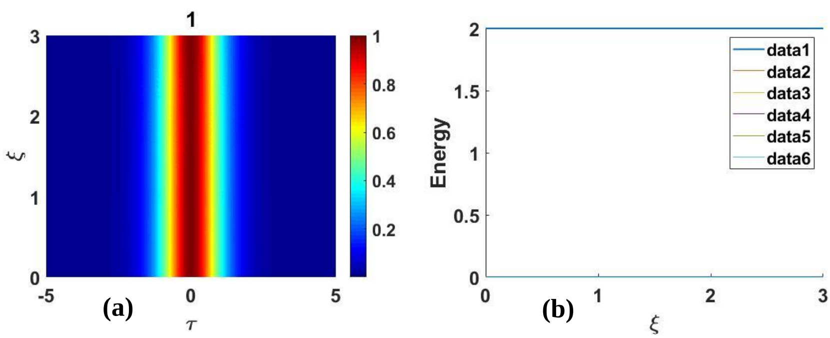


**Fig. 3.** Fundamental soliton is only entered in $LP_{01x}$ mode and no soliton is entered in the other modes. a) temporal density propagation of normalized power $|u^2|$ for fundamental soliton in $LP_{01x}$ mode in terms of normalized fiber length. b) Normalized energy diagram of soliton modes in terms of normalized fiber length.

If we repeat this for each separate mode, the same result is achieved, and no energy exchange takes place. Therefore, if soliton propagation only from one mode in nonlinear few-mode fiber, the shape of the soliton is preserved, and no interaction takes place. In the following by considering one for amplitude of input for $LP_{01}$ and $LP_{11}$ and considering zero for other amplitudes, we investigate soliton propagation and energy in modes. Figs. 4 (a), (b) and (c) show the temporal propagation of power density in modes $LP_{01x}$, $LP_{11ax}$ and $LP_{11bx}$, respectively. But unlike the previous case, the transfiguration of the solitons is well visible, and even for the case (c) where the input is zero, pulse propagation is observed.

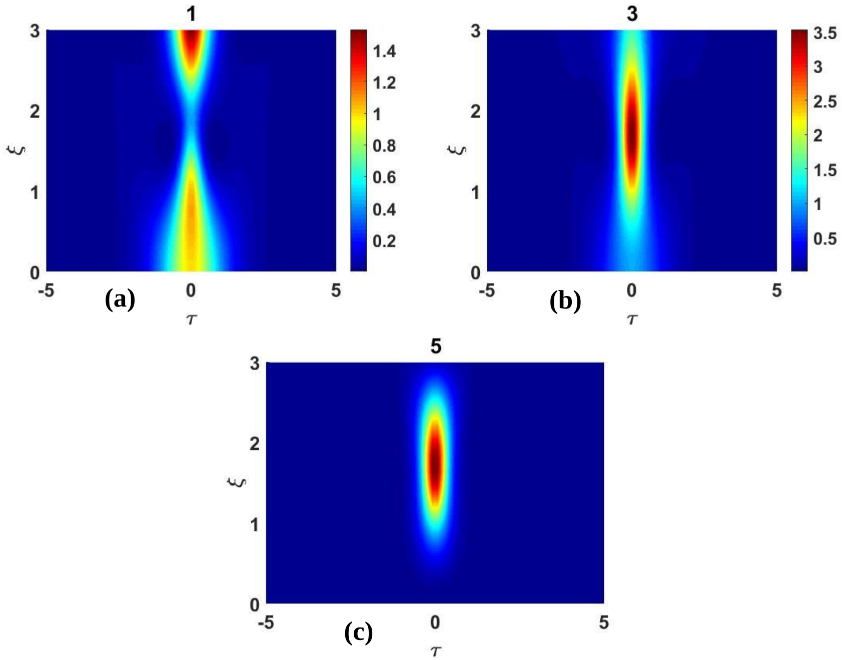


**Fig. 4.** Temporal distribution of normalized power density $|u^2|$ fundamental soliton. a) in $LP_{01x}$ mode b) $LP_{11ax}$ fundamental soliton is only lunched in $LP_{01x}$ and $LP_{11ax}$ modes and no solitons are lunched in the other modes. c) corresponds to the $LP_{11bx}$ mode. Although no soliton has entered in this mode and the input is zero, but we will have a pulse propagation.

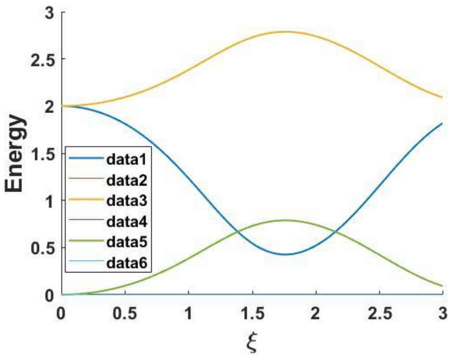


**Fig. 5.** Normalized energy diagram of soliton modes and their interaction with each other. fundamental soliton is only lunched in $LP_{01x}$ and $LP_{11ax}$ modes, and no solitons are lunched in the other modes.

Fig. 5 shows that, the energies of the modes and their energy interaction during propagation. Initially, the energy is transferred from $LP_{01x}$ to the $LP_{11ax}$ and $LP_{11bx}$ and reaches its maximum value at ξ = 1.77 and then the energy is returned, and this process continues. In this exchange, the $LP_{01x}$ energy does not reach zero. It should be noted that these interactions occur between the x components of the fiber modes and have no effect on the y components. If the same simulation is performed for the corresponding modes in y, the result will be the same. Now we consider amplitude 1 for all input modes with polarization x and the results are shown in Fig. 6. As shown in Fig. 6 at first the pulse width decreases in the time domain and its peak increases and reaches its maximum at ξ = 0.82.

However, it gradually loses its energy and its amplitude decreases, and also returns to its original state during propagation, and then this process is repeated. In Fig. 6 (a) the intensity of the pulse peak is higher than in case (b) and (c) and the decrease in pulse width is greater. Also, the pulse peak will increase more sharply while in state (b) and (c) The pulse width gradually decreases. Also, because of the two modes $LP_{11ax}$ and $LP_{11bx}$ are degenerate, the pulse propagation will be the same. Fig. 7, shows the energies of the modes and their interaction of energy during propagation. Initially, energy is transferred to $LP_{01x}$ mode from $LP_{11ax}$ and $LP_{11bx}$modes. The maximum energy exchange between the two modes is at ξ = 0.82. At ξ = 1.56 the energies return to their original state and this process continues.

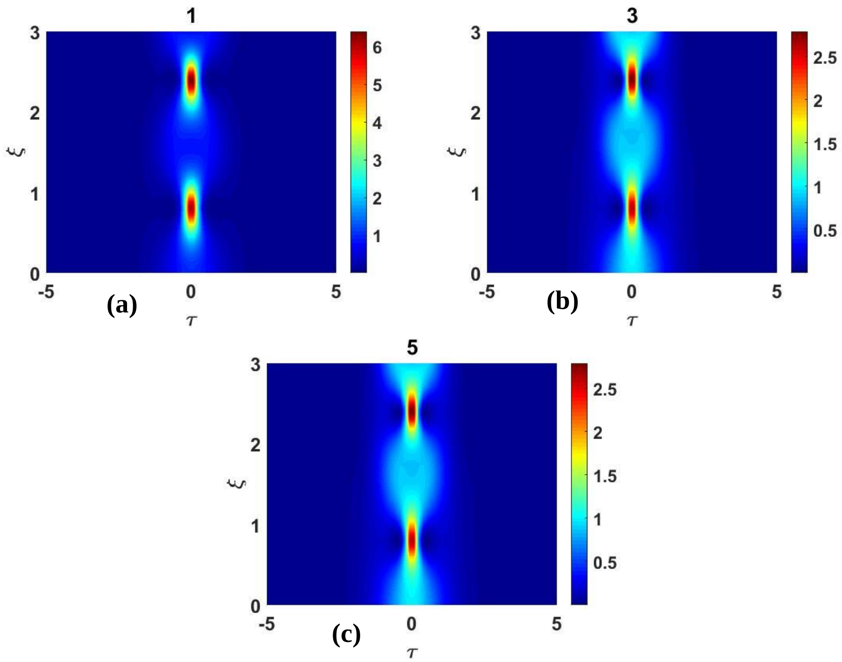


**Fig. 6.** Temporal distribution of normalized power density $|u^2|$ fundamental soliton. a) in $LP_{01x}$ mode b) $LP_{11ax}$ c) $LP_{11bx}$ **.** fundamental soliton is only lunched in $LP_{01x}$ , $LP_{11ax}$ and $LP_{11bx}$modes and no solitons are lunched in the other modes.

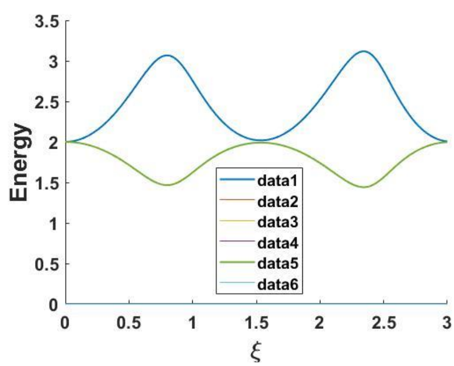


**Fig. 7**. Normalized energy diagram of soliton modes and their interaction with each other. fundamental soliton is only lunched in $LP_{01x}$ , $LP_{11ax}$ and $LP_{11bx}$ modes, and no solitons are lunched in the other modes.

Table IV shows that the power input and phase of each fiber modes for simulation. We propagate solitons in the modes $LP_{01x}$, $LP_{11ax}$, $LP_{11bx}$ and then applied phases $\pi/4$, $\pi/2$, $\pi$ to the mode $LP_{11ax}$, and finally compared the interaction of the modes in these cases.

**TABLE IV**
**POWER INPUT AND PHASE OF EACH FIBER MODE**

| Mode | Input without phase | Input with phase $\pi/4$ | Input with phase $\pi/2$ | Input with phase $\pi$ |
|---|---|---|---|---|
| $LP_{01x}$ | sech $\tau$ | sech $\tau$ | sech $\tau$ | sech $\tau$ |
| $LP_{01y}$ | 0 | 0 | 0 | 0 |
| $LP_{11a\,x}$ | sech $\tau$ | $e^{\frac{i\pi}{4}}$ sech $\tau$ | $e^{\frac{i\pi}{2}}$ sech $\tau$ | $e^{i\pi}$ sech $\tau$ |
| $LP_{11a\,y}$ | 0 | 0 | 0 | 0 |
| $LP_{11b\,x}$ | sech $\tau$ | sech $\tau$ | sech $\tau$ | th $\tau$ |
| $LP_{11b\,y}$ | 0 | 0 | 0 | 0 |

Fig. 8 shows two examples of soliton propagation in the time domain for the $LP_{11a\,x}$ mode in both phaseless and $\pi$-phase modes. Fig. 8(a) is soliton propagation for zero phase. As shown, firstly the pulse width decreases in the time domain and its peak increases and reaches its maximum at ξ = 0.9. However, it gradually loses its energy and its amplitude decreases, and returns to its original state during propagation, and then the process is repeated. But for Fig. 8(b) the pulse peak gradually decreases and reaches its minimum value at ξ = 1.4 and then increases and reaches its maximum value at ξ = 1.8.

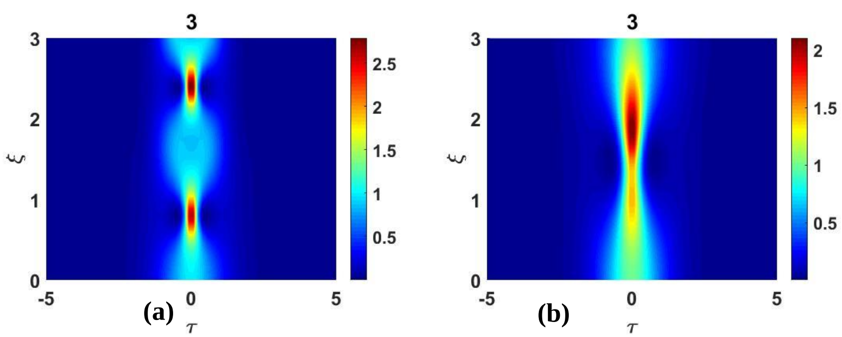


**Fig. 8.** shows the propagation of soliton in $LP_{11ax}$ in state (a) without phase, and (b) with phase $\pi$, respectively.

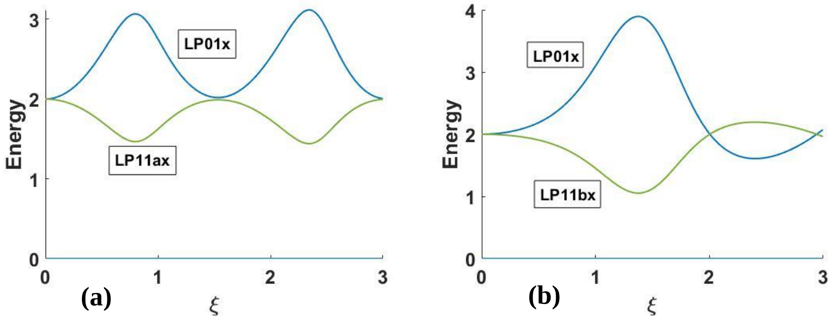


**Fig. 9.** Diagram of modes energy and their interaction with each other by applying phase to $LP_{11a\,x}$. a) Phaseless mode. b) by applying phase π.

In Fig. 9, as an example, the energy of solitons released in $LP_{11a\,x}$ is plotted without phase difference and with phase difference π.

As shown in the figure, the maximum energy exchange between the two modes has taken place at $\xi = 0.9$, but for the π phase at $\xi = 1.4$, the maximum energy exchange has taken place. This indicates that at a certain distance with two phase differences we will have two different forms of energy exchange, which means switching based on the phase difference without electrical effect and is practically an all-optical switching. By various values of phase, the first maximum energy transfer between modes is calculated. We find minimum normalized length 0.66 which equal to a length of 23.3 meters of silica fiber for energy exchange. Unlike couplers, energy exchange takes place through the nonlinear XPM effect, and this effect makes it possible for a single fiber to exchange energy alone, unlike the linear state in modes.

## CONCLUSION

In this paper we simulate the soliton propagation in a few mode silica fibers. The energy exchange between modes is studied extensively. Also, the effect of phase of soliton is investigated. Here we show that the nonlinear effect can cause energy transfer from one mode to another, and this energy transfer depends on the phase. By various values of phase, the first maximum energy transfer between modes is calculated. We find minimum normalized length 0.66 which equal to a length of 23.3 meters of silica fiber for energy exchange. The energy exchange can be used as a basis for all-optical switching.

## REFERENCE


[1] G. P. Agrawal , *Nonlinear Fiber Optics, 6nd*, Academic Press 2019.

[2] G. P. Agrawal, "*Fiber-Optic Communication Systems,* " *4nd*, Wiley & Sons 2013.

[3] W. H. Renninger and F. W. Wise, "*Optical solitons in graded-index multimode fibers*", Nat. Commun. 4(1) (2013)1-6.

Available: https://doi.org/10.1364/PRJ.7.000187

[4] L. G. Wright, W. H. Renninger, D. N. Christodoulides, and F. W. Wise, "*Spatiotemporal dynamics of multimode optical solitons*", Opt. Express 23(3) (2015) 3492-3506. Available: https://doi.org/10.1364/OE.23.003492

[5] K. Krupa, A. Tonello, B. M. Shalaby, M. Fabert, A Barth´el´emy. G. Millot, S. Wabnitz, and V. Couderc, "*Spatial beam self-cleaning in multimode fibers*", Nat. Photon. 11(4) (2017)237-241.

Available: https://doi.org/10.1038/nphoton.2017.32

[6] A. S. Ahsan and G. P. Agrawal, *"Graded-index solitons in multimode fibers*", Opt. Lett. 43(14) (2018) 3345-3348.

Available: https://doi.org/10.1364/OL.43.003345

[7] D.J. Richardson, J. M. Fini, and L.E. Nelson. "*Space-division multiplexing in optical fibers*", Nat. Photonics7(5) (2013) 354-362.

Available: https://doi.org/10.1038/nphoton.2013.94

[8] A. Mafi., "*Pulse Propagation in a Short Nonlinear Graded-Index Multimode Optical Fiber*", Lightwave Technol, 30(17) (2012) 2803-2811.

Available: 10.1109/JLT.2012.2208215

[9] W.H. Renninger, and F.W. Wise, "*Optical solitons in graded-index multimode fibres*", Nat. Commun, 4(1) (2013) 1-6.

Available: https://doi.org/10.1038/ncomms2739

[10] S. Mumtaz, R.J. Essiambre, and G.P. Agrawal, "*Nonlinear propagation in multimode and multicore fibers: Generalization of the manakov equations*", Lightwave Technol J. 31(3) (2013) 398-406.

Available: 10.1109/JLT.2012.2231401

[11] F. Poletti, and p. Horak, J. Opt, "*Description of ultrashort pulse propagation in multimode optical fibers*", JOSA B 25(10) (2008)1645-1654. Available: https://doi.org/10.1364/JOSAB.25.001645

[12] G. P. Agrawal and SH. Buch, "*Soliton stability and trapping in multimode fibers*", *Optics Letters,* 40(2015), 225-228. Available: Available: https://doi.org/10.1364/OL.40.000225

[13] A. Antikainen, L. Rishøj, B.Tai, S.Ramachandran, G. P. Agrawal, "*Fate of a Soliton in a High Order Spatial Mode of a Multimode Fiber*", Physical Review Letters122(2) (2019) 023901. Available: https://doi.org/10.1103/PhysRevLett.122.023901

[14] L. Safaei, M. Borhani zarandi , M. Hatami, "*Effect of Relative Phase on the Stability of Temporal Bright Solitons in a PT- Symmetric NLDC*." Journal of Optoelectronical Nanostructures **3**(3) (2018) 37-46. Available: http://jopn.miau.ac.ir/article_3044.html

[15] M .Dehghani, M. Hatami, A. Gharaati ,. "*Supercontinuum Generation in Silica Plasmonic Waveguide by Bright Soliton*." Journal of Optoelectronical Nanostructures 6(4) (2021) -. Available:10.30495/jopn.2022.28937.1236

[16] M. Rezvani, and M. Fathi Sepahvand. "*Simulation of Surface Plasmon Excitation in a Plasmonic Nano-Wire Using Surface Integral Equations*." Journal of Optoelectronical Nanostructures **1**(1) (2016) 51-64. Available: http://jopn.miau.ac.ir/article_1815.html

[17] A. Keshavarz and Z. Abbasi. "*Spatial soliton pairs in an unbiased photovoltaic-photorefractive crystal circuit*." Journal of Optoelectronical Nanostructures **1**(1) (2016) 81-90. Available: http://jopn.miau.ac.ir/article_1817.html

[18] M.A Sharif,. "*Temporal Nonlinear Dynamics of Plasmon-Solitons, a Duffing Oscillator-Based Approach*." Journal of Optoelectronical Nanostructures **6**(1) (2021)87-102. Available: 10.30495/jopn.2021.4542

[19] M. Ilchi-Ghazaani,. "*Analysis of Steady-State Brillouin Nonlinearity in High-Power Fiber Lasers.*" Journal of Optoelectronical Nanostructures 5(3) (2020)1-16. Available: http://jopn.miau.ac.ir/article_4401.html

[20] V. Fallahi, and M. Seifouri. "*Novel structure of optical add/drop filters and multi-channel filter based on photonic crystal for using in optical telecommunication devices.*" Journal of Optoelectronical Nanostructures 4(2) (2019) 53-68. Available: http://jopn.miau.ac.ir/article_3478.html

[21] B.E. Saleh and M.C Teich, "*Fundamentals of photonics*", 2nd, Wiley, New York, 2007.